

Supporting information for

**Microstructural control and selective C<sub>2</sub>H<sub>5</sub>OH sensing properties of Zn<sub>2</sub>SnO<sub>4</sub> nanofibers prepared by electrospinning”**

**Seung-Hoon Choi<sup>a</sup>, In-Sung Hwang<sup>b</sup>, Jong-Heun Lee<sup>b</sup>, Seong-Geun Oh<sup>a</sup>,  
and Il-Doo Kim<sup>c,\*</sup>**

<sup>a</sup>Department of Chemical Engineering, Hanyang University, Seoul 133-791, Republic of Korea

<sup>b</sup>Department of Materials Science and Engineering, Korea University, Anam-Dong, Seongbuk-Gu, Seoul 136-713, Republic of Korea

<sup>c</sup>Department of Materials Science and Engineering, Korea Advanced Institute of Science and Technology, Daejeon 305-701, Republic of Korea

**Experimental Section**

**Preparation of Zn<sub>2</sub>SnO<sub>4</sub> nanofibers:**

Poly(vinyl acetate) (PVAc, M<sub>w</sub>=1,300,000 mol/g) was synthesized using bulk radical polymerization. Poly(vinyl pyrrolidone) (PVP, M<sub>w</sub>=1,300,000 mol/g), Zn(CH<sub>3</sub>COO)<sub>2</sub>·2H<sub>2</sub>O (99%+) and Sn(CH<sub>3</sub>COO)<sub>4</sub> (99%+) were purchased from Aldrich. Anhydrous N,N-dimethylformamide (DMF) was obtained from J.T Baker. The chemical reagents were used without further purification.

For the synthesis of porous Zn<sub>2</sub>SnO<sub>4</sub> fibers, the precursor solution for electrospinning was prepared by dissolving 1.756 g of Zn(CH<sub>3</sub>COO)<sub>2</sub>·2H<sub>2</sub>O, 1.42 g of Sn(CH<sub>3</sub>COO)<sub>4</sub> and 1.5 g of PVAc in 15.8 ml of DMF. To obtain dense Zn<sub>2</sub>SnO<sub>4</sub> fibers, the precursor solution for electrospinning was prepared by dissolving 1.317g of Zn(CH<sub>3</sub>COO)<sub>2</sub>·2H<sub>2</sub>O, 1.065 g of Sn(CH<sub>3</sub>COO)<sub>4</sub> and 1.3 g of PVP in 7.2 ml of DMF. In order to minimize formation of undesirable crystalline phases such as ZnO or SnO<sub>x</sub>, a precursor solution with a stoichiometric ratio was carefully mixed and processed. During the electrospinning process the solution was injected through a stainless steel needle (25 gauge, orifice diameter = 250 μm) that was connected to a high-voltage DC power supply (Bertan, High-voltage power supply series 230). The solution was continuously fed through the nozzle using a syringe pump (KD scientific, 781200) at a rate of 20 μL/min. High voltage

(17.2 kV) was applied between the needle and the grounded collector, located 15 cm below the needle. At the initial stage of electrospinning, a fiber stream ejected from a positively charged Talyor cone formed at the nozzle tip, undergoes the solidification followed by phase separation between the organic polymer and inorganic precursors. In the case of the highly immiscible inorganic precursor/polymers system, fast phase separation and solidification occur during solvent vaporization, resulting in the formation of inhomogeneous composite fibers composed of inorganic precursor rich and polymer rich domains. Individual domains co-exist, allowing domain elongation in liquid phases. On the other hand, in the case of the highly miscible precursor and polymer system, phase separation was not generated, leading to homogeneous composite fibers. Thus, after heat treatment, two different fiber morphologies, i.e., highly porous or very dense fibers, can be formed (see details in Fig. S1). In this work, a continuous Zn, Sn precursor/PVAc (or PVP) fiber stream was ejected from the nozzle as a long fiber and was collected on the substrate (a stainless steel plate). Subsequently, the samples were calcined at 700 °C for 1 hr in air to remove the organic constituents of the matrix polymer of PVAc or PVP. The fiber diameter can be tuned by tailoring the electrospinning conditions, i.e., solution viscosity, flow rate of solution and the distance between the nozzle and the collector. SiO<sub>2</sub>(300nm)/Si wafers were used as substrates in specimens for microstructural characterizations.

### Gas sensing characteristics:

For the formation of the sensing layer, porous and dense Zn<sub>2</sub>SnO<sub>4</sub> fibers were made in a paste form and applied to alumina substrates fitted with an interdigitated gold electrode (2 fingers, 900 µm long and 600 µm wide, spaced 100 µm apart). Finally, the sensor layer was heat-treated at 550°C for 1h to decompose the organic content of the paste. Prototype gas sensors utilizing porous and dense Zn<sub>2</sub>SnO<sub>4</sub> fibers, i.e. a nanorod structure with high aspect ratio, are well interconnected. The sensor was placed in a quartz tube and the temperature of the furnace was stabilized at 450°C. The gas concentration was controlled by changing the mixing ratio of 100 ppm gases (H<sub>2</sub>, CO and C<sub>2</sub>H<sub>5</sub>OH; in air balance) and employing dry synthetic air. A flow-through technique with a constant flow rate of 500 cm<sup>3</sup>/min used. The gas response ( $S=R_a/R_g$ , R<sub>a</sub>:resistance in air, R<sub>g</sub>: resistance in gas) was measured at 450°C. The dc 2 probe resistance of the sensor was measured using an electrometer interfaced with a computer.

### **Characterization:**

The morphology and microstructural evolution were examined by field emission scanning electron microscopy (FE-SEM, JEOL JSM 6330F). A focused ion beam (FIB, NOVA 600, FEI) was used to cut sharp cross sections of the composite fibers calcined at different temperatures for closer examination of their inner morphology. Scanning transmission electron microscopy (STEM) and high-resolution TEM (HR-TEM, Tecnai G2 (FEI)), equipped with an energy dispersion spectrometer (EDS), were used for the microstructural and chemical composition analyses of the prepared fibers. Thermogravimetric studies were carried out using a TG-2050 thermal analyzer system (Ta instruments, Inc.) X-ray diffraction (XRD) was used to examine the phase composition of fiber mats. The surface areas of the  $Zn_2SnO_4$  fibers were investigated using the Brunauer-Emmett-Teller (BET) method (Belsorpmini, BEL Japan Inc.)

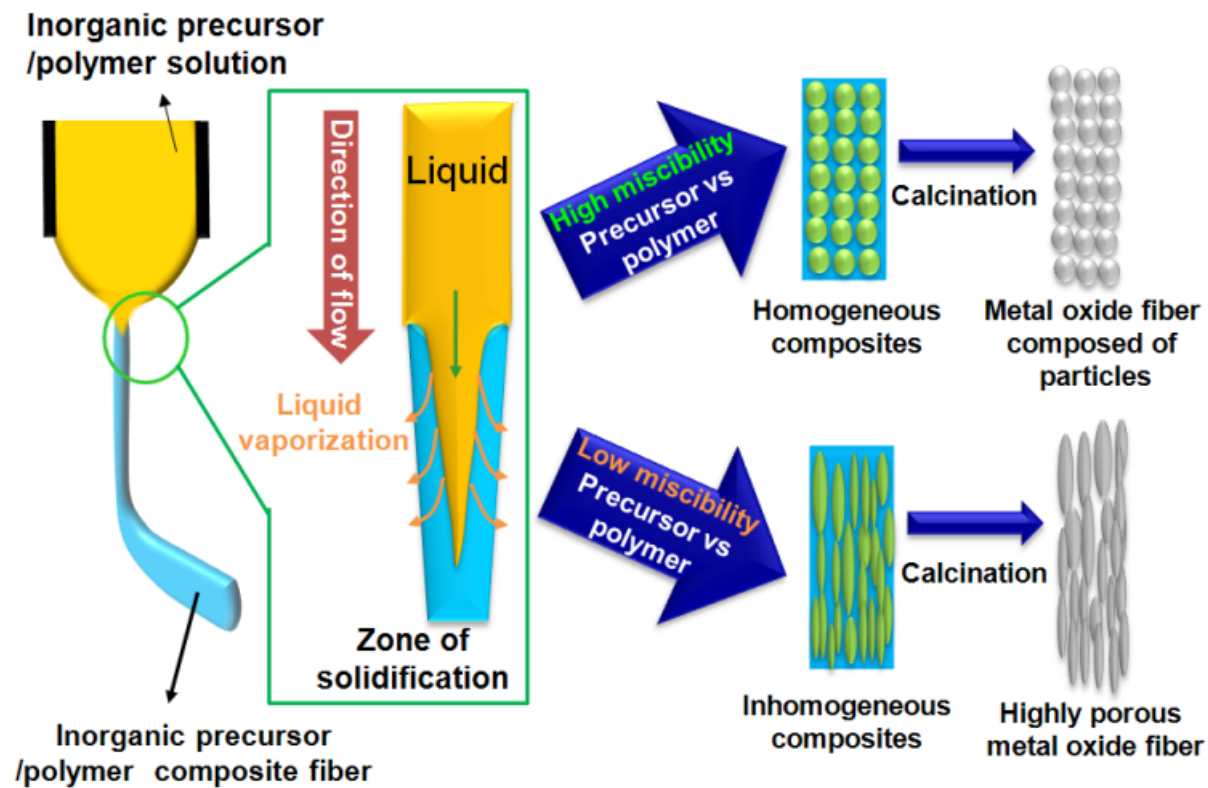


**Fig. S1** Schematic formation mechanism of polycrystalline  $\text{Zn}_2\text{SnO}_4$  nanofibers with different morphologies via electrospinning of the inorganic precursor/polymer solution.

-SEM cross sectional images of single fiber from each calcination step using FIB milling

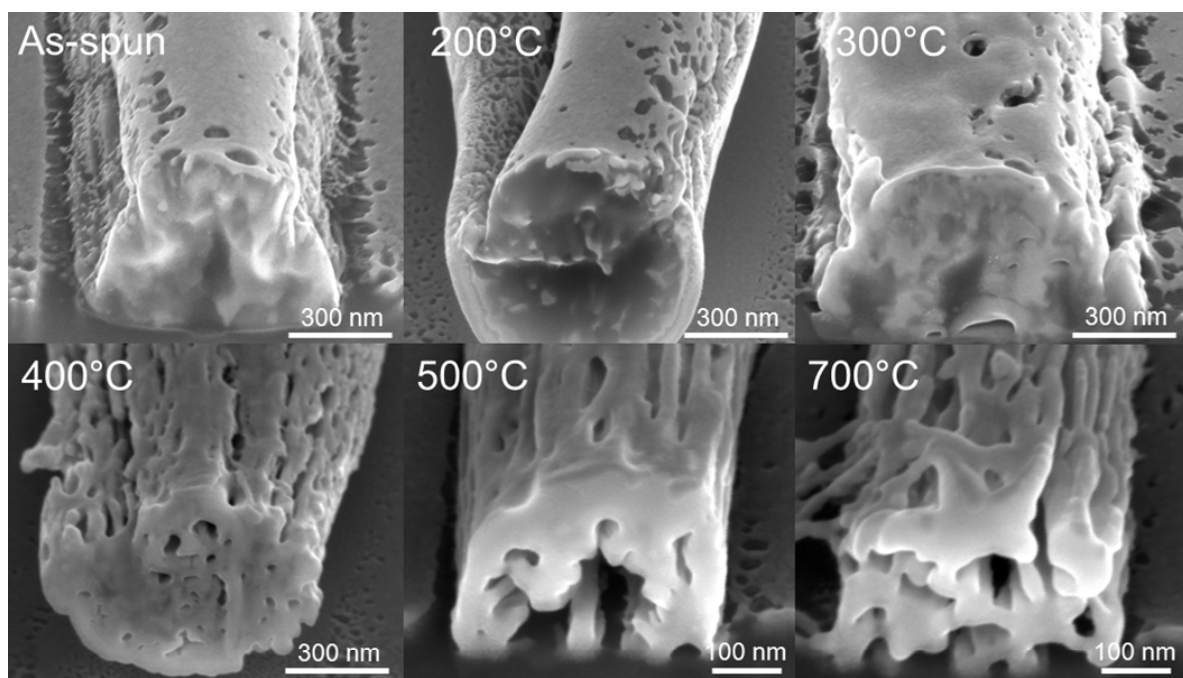


**Fig. S2** FESEM cross-sectional images of single Zn(OAc)<sub>2</sub>-Sn(OAc)<sub>4</sub>/PVAc composite fiber and heat-treated Zn<sub>2</sub>SnO<sub>4</sub> fibers at different temperatures. Focused-ion beam milling process was used for characterization of the cross-sectional view.

## -Thermal behavior and microstructure analysis of Zn(OAc)<sub>2</sub>-Sn(OAc)<sub>4</sub>/PVP composite fibers using TGA and FIB-SEM

In order to clearly examine the microstructural evolution of the inner morphology of dense Zn<sub>2</sub>SnO<sub>4</sub> fibers as a function of annealing temperature, we carried out thermal gravimetric analyses (TGA) and focused ion beam (FIB)-SEM analyses on the Zn(OAc)<sub>2</sub>-Sn(OAc)<sub>4</sub>/PVP composite fibers. Fig. S3 shows a representative TGA curve of Zn(OAc)<sub>2</sub>-Sn(OAc)<sub>4</sub>/PVP composite fibers and longitudinal and cross section images of a FIB-cut single fiber after each calcination step. As indicated in the cross-sectional inset image of Fig. S3, as-spun Zn(OAc)<sub>2</sub>-Sn(OAc)<sub>4</sub>/PVP composite fibers are composed of a homogeneous mixture (Fig. S3a). Below 300°C, residual DMF and water in the as-spun fibers were slowly vaporized (region I in Fig. S3). The degradation process of the composite fibers shows two main distinctive regions (II-1 and II-2 regions in Fig. S3). In the first step, the composite fibers begin to lose weight at around 300°C and weight loss continues up to 350°C (region II-1 in Fig. S3), which indicates the thermal decomposition of organic group mostly associated with acetate group of Zn(OAc)<sub>2</sub>-Sn(OAc)<sub>4</sub> and the degradation of pyrrolidone groups in PVP. When the decomposition temperature (300°C) is first reached, the inner morphologies of the solid-state Zn, Sn precursors maintained their initial shape (Fig. S3b). As the temperature is increased to 500°C, the unsaturated carbon backbone and residual organic composites burned out (region II-2 in Fig. S3) and the Zn-Sn precursor was crystallized, retaining its dense inner morphology (Fig. S3c and S3d). The dense morphology remains unchanged after heat-treatment at 700°C (region III in Fig. S3 and Fig. S3e).

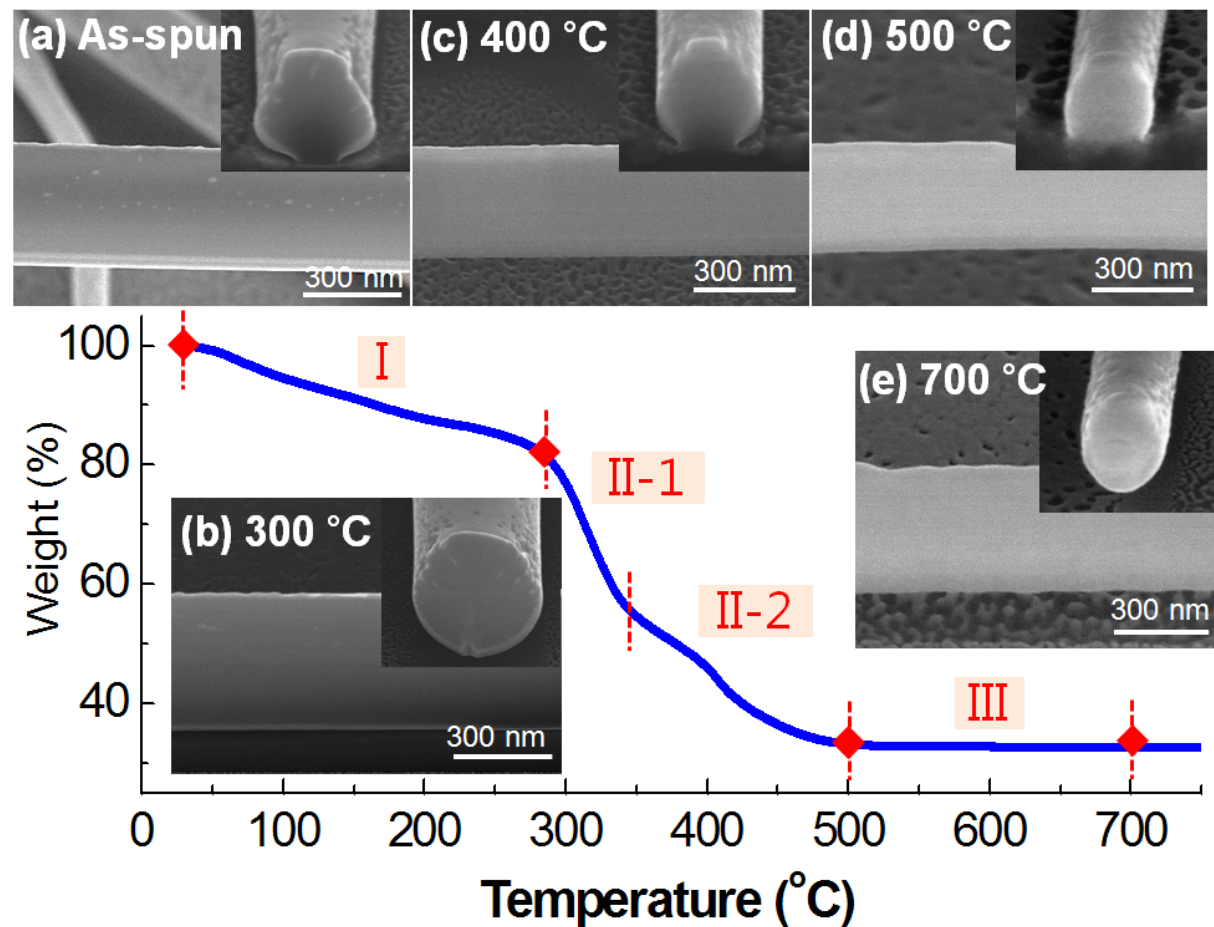


**Fig. S3** TGA curve of  $\text{Zn}(\text{OAc})_2\text{-Sn}(\text{OAc})_4/\text{PVP}$  composite fibers; inset shows FESEM longitudinal and cross-sectional images of single fiber taken from each calcination step of 10 mins each using FIB milling.

**-Investigation on the surface areas of porous and dense Zn<sub>2</sub>SnO<sub>4</sub> fibers using BET method**

Figure S4 compares the N<sub>2</sub> adsorption-desorption isotherms and the pore size distribution of the porous and dense Zn<sub>2</sub>SnO<sub>4</sub> fibers and demonstrates much larger accessible pore volume of the porous Zn<sub>2</sub>SnO<sub>4</sub> fibers. According to the IUPAC classification, the N<sub>2</sub> adsorption-desorption isotherm curves resemble the type IV with type H5 hysteresis loops, which are typical for mesoporous materials. There are dissimilarities between the two N<sub>2</sub> adsorption-desorption isotherms, possibly due to the different nanochannel structure of Zn<sub>2</sub>SnO<sub>4</sub> fibers. The multi-modal distribution of small pores in the porous Zn<sub>2</sub>SnO<sub>4</sub> fibers, with peaks at approximately 5 ~ 20 nm, can be correlated to their unique morphology, as illustrated in inset of Fig. S4. Various size of small pores are found among the highly porous surface and lotus-root-like inner structure (Figs. 1c and 1d). From the dense Zn<sub>2</sub>SnO<sub>4</sub> fibers, on the other hand, a narrow pore distribution in a range of 5 ~ 15 nm is observed (Fig. 1i). Meanwhile, the pore volumes for the porous and dense Zn<sub>2</sub>SnO<sub>4</sub> fibers are estimated to be 0.057 and 0.018 mL/g, respectively. The multi-modal distribution in the porous Zn<sub>2</sub>SnO<sub>4</sub> fibers appears to serve the dual needs for rapid gas diffusivity and high sensitivity. Thus, the combination of enhanced surface area and high porosity of porous Zn<sub>2</sub>SnO<sub>4</sub> fibers is expected to lead to exceptionally high gas sensitivity as compared to that of dense Zn<sub>2</sub>SnO<sub>4</sub> fibers.

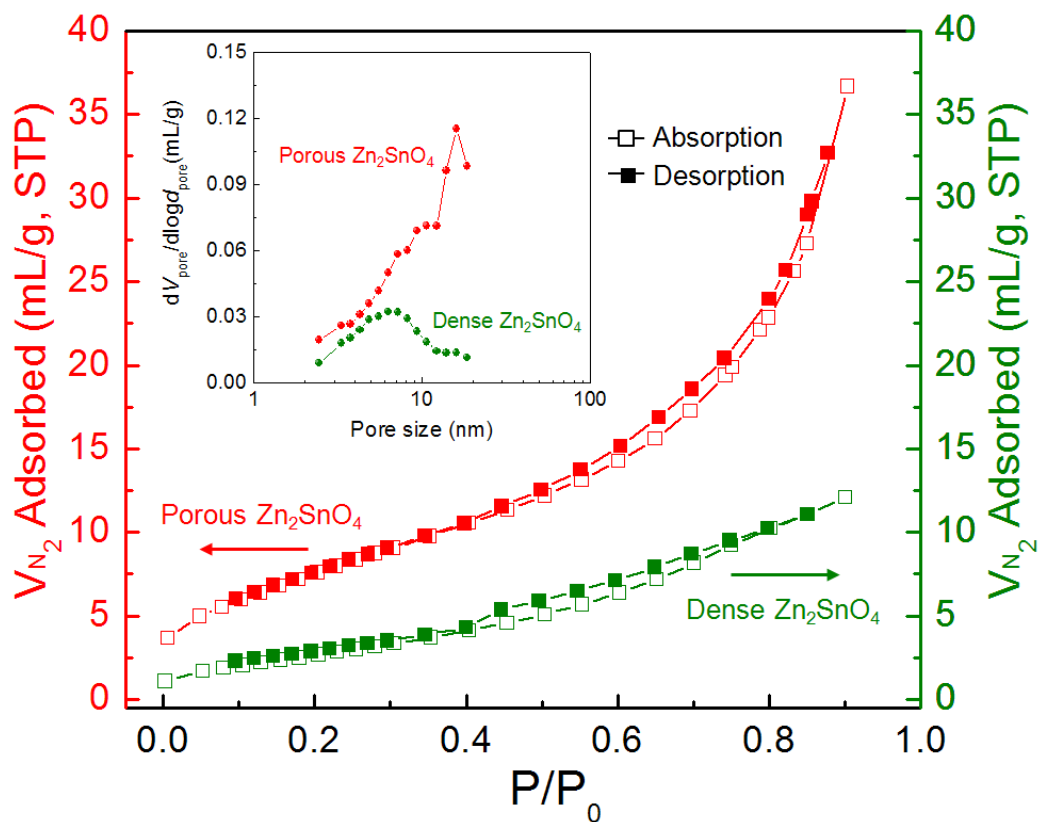


**Fig. S4** N<sub>2</sub> adsorption-desorption isotherms; inset shows BJH pore-size distribution plots of the Zn<sub>2</sub>SnO<sub>4</sub> fibers.